https://doi.org/10.15407/ujpe70.6.381

G. NURMURODOVA,[1] I. DOROSHENKO,[1,2] G. MURODOV,[1] U. KHUJAMOV[1]

[1] Institute of Engineering Physics, Samarkand State University named Sharof Rashidov
(Uzbekistan; e-mail: gnurmuradava@gmail.com)
[2] Taras Shevchenko National University of Kyiv
(64/13, Volodymyrska Str., Kyiv 01601, Ukraine)

FTIR AND DFT STUDY OF $(CH_3)_2CO\cdots HCl$ HYDROGEN-BONDED COMPLEX

The study of hydrogen-bonded complexes is crucial for understanding intermolecular interactions that influence molecular structure, electron density distribution, and vibrational properties. In this work, we will investigate the acetone-hydrogen chloride $(CH_3)_2CO\cdots HCl$ complex using Fourier-transform infrared (FTIR) spectroscopy in cryogenic krypton and xenon solutions, alongside density functional theory (DFT) calculations. The experimental IR spectra reveal characteristic frequency shifts upon the complex formation, while the computational analysis provides insights into geometric and electronic structure changes. Topological analyses, including Atoms in Molecules (AIM) and Non-Covalent Interaction (NCI) approaches, confirm the presence and strength of hydrogen bonding. The study highlights solvent effects on vibrational properties and intermolecular interactions, advancing the understanding of the hydrogen bonding in complex molecular systems.

Keywords: $(CH_3)_2CO\cdots HCl$ complex, IR spectrum, hydrogen bonding, AIM, RDG, NCI.

1. Introduction

Experimental and theoretical studies of hydrogen-bonded complexes play an important role in modern physics, chemistry, biology, and many other fields [1–5]. Forces of intermolecular interaction have a significant effect on the structure, electron density distribution, vibrational properties, and many other dynamic parameters of molecules. In liquid systems containing different types of molecules the situation is more complicated due to the solution effect. In this regard, the impact of "solvation" on the vibrational properties of molecules may be studied using vibrational spectroscopy and quantum-chemical simulation [6, 7]. Studying how solvents affect molecules is crucial, since the majority of biochemical reactions take place in the solution phase [8, 9]. IR absorption spectroscopy is one of the most convenient methods that provide the detailed information about intermolecular interactions [10–12]. In our research work, FTIR spectroscopy is used to study the mechanism of interaction between molecules of acetone, hydrogen chloride, and their binary complexes. Experimentally obtained vibrational spectra of these complexes allow determining a set of electro-optical parameters and confirming the correctness of the calculation methods.

The 1 : 1 complex of acetone and hydrogen chloride ($(CH_3)_2CO\cdots HCl$) contains proton donor (HCl) and proton acceptor (CO) groups, which form an impor-

Citation: Nurmurodova G., Doroshenko I., Murodov G., Khujamov U. FTIR and DFT study of $(CH_3)_2CO\cdots HCl$ hydrogen-bonded complex. *Ukr. J. Phys.* **70**, No. 6, 381 (2025). https://doi.org/10.15407/ujpe70.6.381.

tant hydrogen-bonded system that can be studied experimentally and theoretically. Some thermodynamic and spectroscopic properties of the $(CH_3)_2CO\cdots HCl$ complex have already been measured by IR spectroscopy and calculated by ab initio methods [13–15]. Nevertheless, peculiarities of intermolecular interaction between hydrogen chloride and acetone molecules have not been sufficiently studied. In our work, a coordinated experimental and theoretical analysis of the IR spectrum of $(CH_3)_2CO\cdots HCl$ complex is performed, ae well as topological analysis of the complex.

2. Methods

FTIR spectra of acetone and hydrogen chloride in cryosolutions with Kr (145 and 160 K) and Xe (170 K) were registered. Low-temperature inert solutions allow studying spectral parameters of individual molecules and complexes due to the absolute transparency of these solvents in the IR range and low interaction of the studied molecules with the solvent. Thus, the IR spectra of acetone and HCl molecules, as well as their 1 : 1 complexes, were obtained using a Bruker IFS-125 HR vacuum Fourier spectrometer in a wide spectral region (4000–900 cm^{-1}) encompassing the C=O and H–Cl fundamental stretching bands. The experiments were performed in a cryostat with a horizontal optical axis and a path length of ∼10 cm. A stainless steel cuvette with two BaF_2 windows is designed to operate at high pressures, which allows changing the temperature of solutions in the range of 120–190 K.

The Density Functional Theory (DFT) method was used to optimize the geometry of $(CH_3)_2CO$ molecule and the complex of $(CH_3)_2CO$ with HCl. The 6–311++G(d,p) basis set was used in the calculations to account for intermolecular interaction as accurately as possible [16–19]. IR frequencies for the monomers and complexes were calculated at the same level of theory. DFT calculations were performed using the Gaussian 09 W software [20]. GaussView 6.0 program was used for the visualization [21]. Additionally, the MULTIWFN [22] software was used to acquire the topological features of the electron density distribution in the most stable structure in order to gain a greater knowledge of intermolecular interactions based on Bader's AIM theory [23]. Non-covalent interaction (NCI) and reduced density gradient (RDG) studies were carried out using VMD [24] software.

3. Results and Discussions

3.1. DFT analysis of the equilibrium geometry

The equilibrium geometries of HCl and $(CH_3)_2CO$ molecules, as well as $(CH_3)_2CO\cdots HCl$ complex, were calculated at B3LYP/6 311++G(d,p) level of theory using the Gaussian 09 package. The calculations were carried out for three different media: vacuum, Kr and Xe environments. In Gaussian software, calculations in vacuum are carried out by default, while the environment was specified in the form of the corresponding solvent in the frame of the polarizable continuum model (PCM) using the normal Solvent option to the SCRF keyword. All the calculations were performed for temperature 298.15 K. The obtained results are presented in Fig. 1. Bond lengths are indicated in Å.

From the results of the calculations, it can be seen that the distance between atoms in the free HCl molecule in vacuum is 1.287 Å, under the influence of solvents (both Kr and Xe) it changed by $\Delta r_{H-Cl} = 0.001$ Å. For the $(CH_3)_2CO$ molecule, under the influence of Kr as a solvent, the bond lengths change by $\Delta r_{C=O} = 0.001$ Å, $\Delta r_{C-C} = -0.001$ Å, and the angle $\alpha_{(C3,C2,C4)}$ by 0.02^0. Under the influence of Xe, the corresponding changes are $\Delta r_{C=O} = 0.002$ Å, $\Delta r_{C-C} = -0.002$ Å, and $\Delta\alpha_{(C3,C2,C4)} = 0.05°$. In the $(CH_3)_2CO\cdots HCl$ complex, along with the effect of the solvents, intermolecular interactions also cause structural parameters changes. In this case, the lengths of the bonds H–Cl, C=O, and C–C change significantly compared to the corresponding lengths in monomers. All calculated structural parameters for $(CH_3)_2CO\cdots HCl$ complexes in different environments are presented in Table 1.

Our calculation on the whole confirms the results of the earlier investigation of acetone-HF complexes [25, 26]. The value of COH angle 126.73° in vacuum, 126.86° in Kr and 127.07° in Xe is in a good agreement with the trigonal structure of the electron cloud of the O atom in this complex. The geometrical parameters ordinarily used to characterize the H-bond have very close equilibrium values in these complexes, namely, $r(HCl) =$ 1.3155, 1.3214, and 1.3230 Å in acetone···HCl complex in vacuum, Kr and Xe, respectively. The corresponding values of $r(Cl\cdots O)$ are 3.1199, 3.0843, and 3.0749 Å. Determined as the difference between the electronic energies of the two monomers in the equilibrium configuration and the

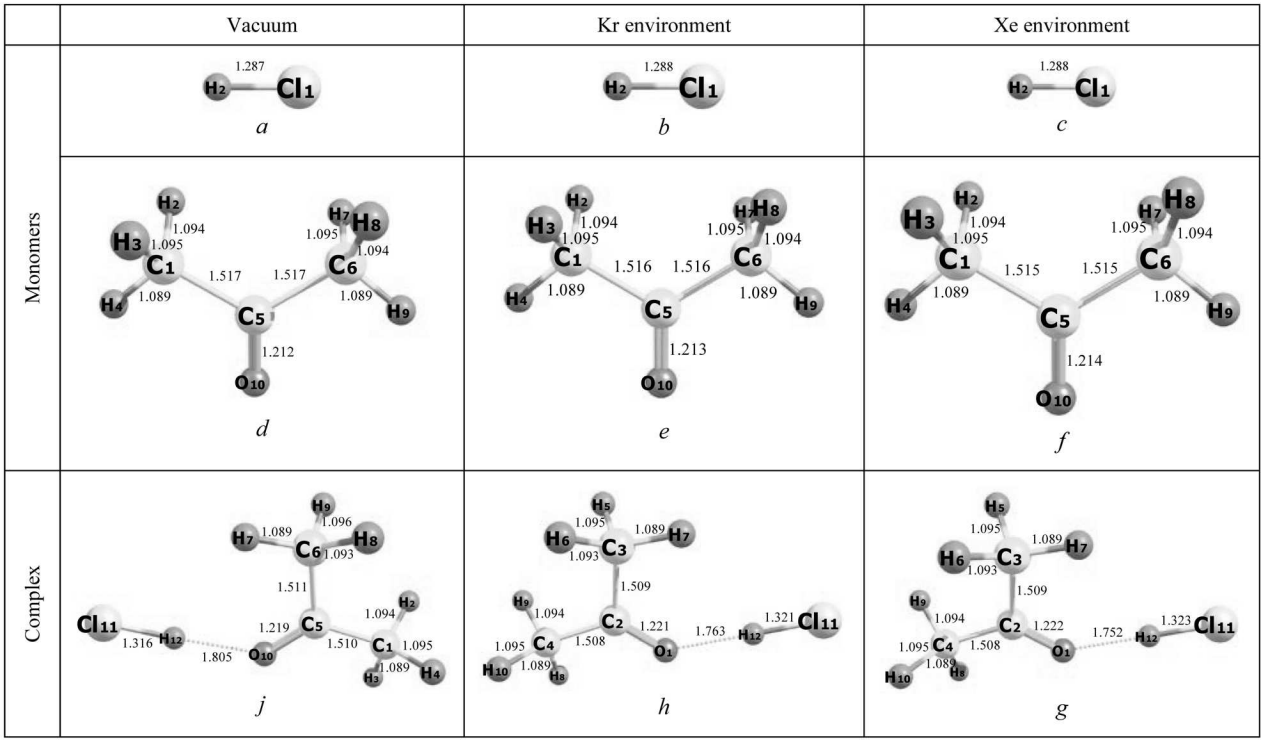

Fig. 1. Calculated optimal structures of free molecules $(CH_3)_2CO/HCl$ and $(CH_3)_2CO\cdots HCl$ complexes in vacuum and in Kr and Xe environments

Table 1. **Calculated structural parameters of the $(CH_3)_2CO\cdots HCl$ complex**

Bond lengths (Å)	C_5O	C_5C_1	C_1H_3	C_1H_4	C_6H_7	C_6H_9	Cl···O	ClH
Vacuum	1.2191	1.5103	1.0888	1.0954	1.0889	1.0956	3.1199	1.3155
Bond lengths (Å)	C_2O	C_2C_4	C_4H_8	C_4H_{10}	C_3H_7	C_3H_5	Cl···O	ClH
Kr Xe	1.2213 1.2218	1.5085 1.5079	1.0887 1.0887	1.0954 1.0953	1.0888 1.0887	1.0954 1.0953	3.0843 3.0749	1.3214 1.3230
Angles (°)	OC_5C_1	OC_5C_6	$H_3C_1C_5$	$H_2C_1C_5$	$ClOC_5$	$C_5C_6H_9$	$OClH_{12}$	C_5OH_{12}
Vacuum	120.68	122.09	110.29	110.84	125.48	108.91	1.73	126.73
Angles (°)	OC_2C_4	OC_2C_3	$H_8C_4C_2$	$H_9C_4C_2$	$ClOC_2$	$C_2C_3H_5$	$OClH_{12}$	C_2OH_{12}
Kr Xe	120.61 120.59	122.09 122.09	110.39 110.42	110.71 110.68	126.85 127.08	108.89 108.89	0.31 0.08	126.86 127.07

equilibrium electronic energy of the complex, the hydrogen bond energies of these complexes in vacuum, Kr, and Xe are –06.73, –6.84, and –6.86 kcal/mol, respectively. We also note that the harmonic frequencies obtained in the space of normal coordinates and assigned to the H–Cl stretching mode are 2545, 2474,

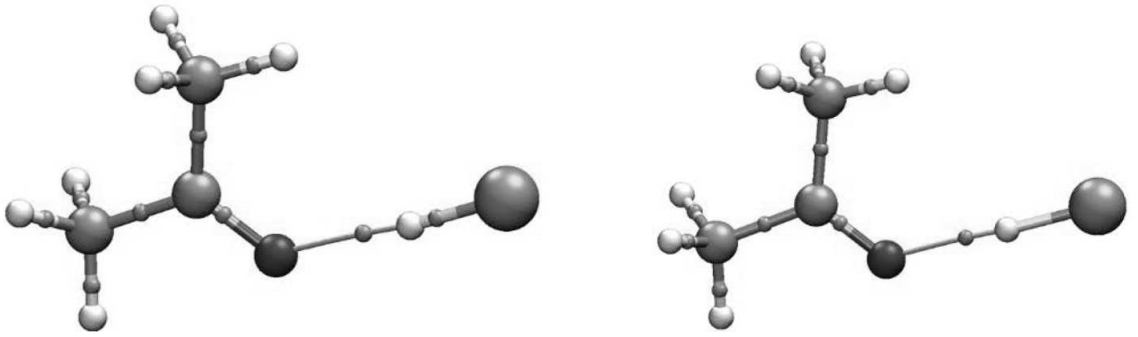

a *b*

Fig. 2. AIM analysis of the $(CH_3)_2CO\cdots HCl$ complex in vacuum (*a*) and in the solution (*b*). Yellow dots represent bonds critical points

Table 2. **Results of AIM analysis: ρ – electron density; $\nabla^2\rho$ – Laplacian of electron density; $G(r)$ – kinetic energy density; $V(r)$ – potential energy density; $H(r)$ – sum of electron density; $E_{\text{int.}}$ – intermolecular interaction energy (kcal/mol)**

Complex	Environment	Hydrogen bond	ρ (a.u)	$\nabla^2\rho$ (a.u)	$G(r)$ (a.u)	$V(r)$ (a.u)	$H(r)$ (a.u)	$E_{\text{int.}}$ (kcal/mol)
$(CH_3)_2CO\cdots HCl$	Vacuum	$O_{10}\cdots H_{12}$	0.035	0.108	0.0268	–0.0265	0.0003	–8.31
	Kr	$O_1\cdots H_{12}$	0.039	0.115	0.0297	–0.0306	–0.0009	–9.6
	Xe		0.040	0.117	0.0305	–0.0318	–0.0013	–9.97

and 2450 cm^{-1} for the above complexes. Judging from these results, one might conclude that the H-bonds in these compounds are very similar [26]. However, as will be shown below, there are significant distinctions between these systems.

3.2. Topological analyses

AIM is performed to find out all interactions, both intramolecular and intermolecular ones (such as the van der Waals interactions and H-bonding) [27]. The AIM analysis is based on bond critical points (BCPs) like electron density (ρ), Laplacian of electron density ($\nabla^2\rho$), and total electron density, which evaluate the bond nature and type. Electron density (ρ) determines the strength of bond, whereas the kinetic energy density, Laplacian ($\nabla^2\rho$), the total electron energy density H, and the potential energy density explain the bond nature. For covalent bonds, the value of the electron density is greater than 0.1 a.u. with a large but negative Laplacian.

Both recent and earlier studies have demonstrated the effectiveness of the AIM technique in examining hydrogen bonding. However, determining the type of covalent interaction requires knowledge of the local electron energy density at the bond critical point (BCP). The nature of the interaction can be characterized using the Laplacian function of the electron density at the hydrogen bond critical point (H_{BCP}), denoted as $\nabla^2\rho_{BCP}$.

Figure 2 presents molecular diagrams of the complexes considered in this study. According to the calculations (see Table 2), the ρ_{BCP} value for the O···H interaction in vacuum is 0.035 a.u., with a corresponding $\nabla^2\rho_{BCP}$ value of 0.108 a.u. When krypton is used as a solvent, these values increase to 0.039 a.u. and 0.115 a.u., respectively. In the presence of xenon, they further rise to 0.040 a.u. and 0.117 a.u. These values align with commonly accepted ranges for hydrogen bonding, indicating a partially covalent nature.

Table 2 also reveals that hydrogen bonds are preserved in all structures, as indicated by the near-zero ellipticity values for O···H interactions. This not only confirms the presence of the hydrogen bonding, but also provides a measure of its strength, given that

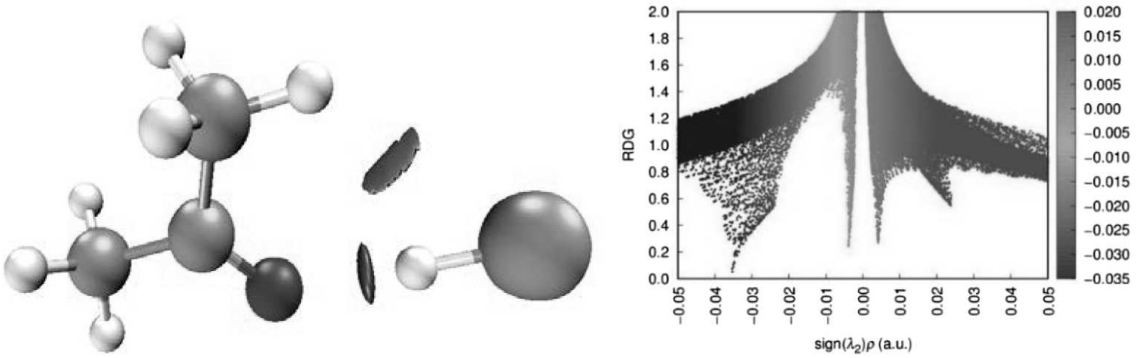

a *b*

Fig. 3. 3D colored isosurface (*a*) and 2D RDG graph of the acetone-HCl complex in vacuum (*b*)

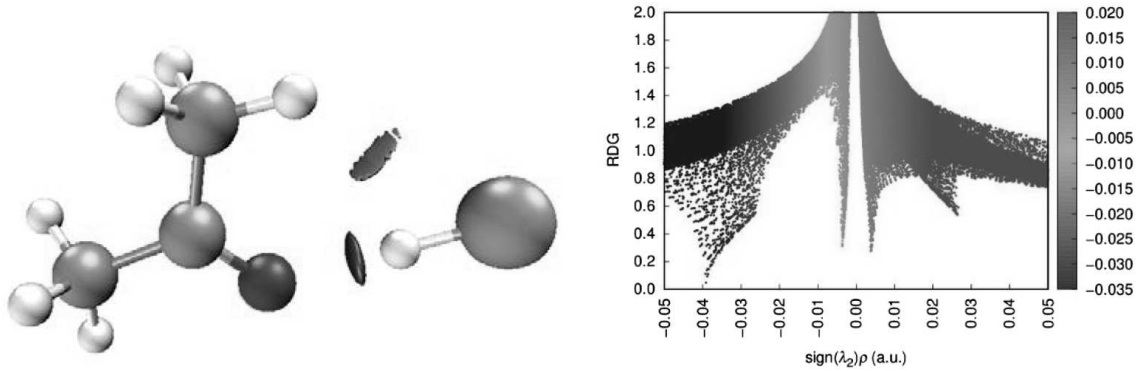

a *b*

Fig. 4. 3D colored isosurface (*a*) and 2D RDG graph of the acetone-HCl complex in Kr (*b*)

electron density at BCP decreases exponentially with distance.

Based on these findings, the interaction energies (E_{int}) for acetone-HCl complexes are –8.31 kcal/mol in vacuum, and –9.6 and –9.97 kcal/mol in krypton and xenon, respectively.

The Laplacian ($\nabla^2\rho$) value is positive for all studied complexes, which indicates the presence of noncovalent interactions between acetone and HCl molecules. This observation is also strongly correlated with the interaction energy analysis. These results help us to determine the interaction energy of the $(CH_3)_2CO\cdots HCl$ complex.

Non-covalent interaction (NCI) analysis andreduced density gradient (RDG) analysis provide insight into non-covalent interactions, present in the complex, including hydrogen bonding, steric repulsions, and van der Waals forces [27–32]. This method is based on the first derivative of the electron density (ρ) and the second eigenvalue of the Hessian matrix, which is why it is referred to as RDG analysis. Figures 3–5 present the results of the NCI analysis, including 3D isodensity plot and 2D RDG representation. Here strong electrostatic interactions (hydrogen bonds) are represented by blue color, repulsion forces are indicated by red color, and weak interactions (van der Waals interactions) are shown by green color.

The 2D RDG graph plots the reduced density gradient (RDG) on the x-axis and $\lambda_2(\rho)$ on the y-axis. In this representation, the sign of $\lambda_2(\rho)$ indicates the nature of the interaction, while ρ provides information about the bond strength. When $\lambda_2(\rho) > 0$, the van der Waals interactions dominate, whereas $\lambda_2(\rho) > 0$ indicates steric repulsions. In the 3D visualization, different colors correspond to $\lambda_2(\rho)$ values: red patches ($\lambda_2(\rho) > 0$) represent steric repulsions, green patches ($\lambda_2(\rho) \approx -0.02$) indicate hydro-

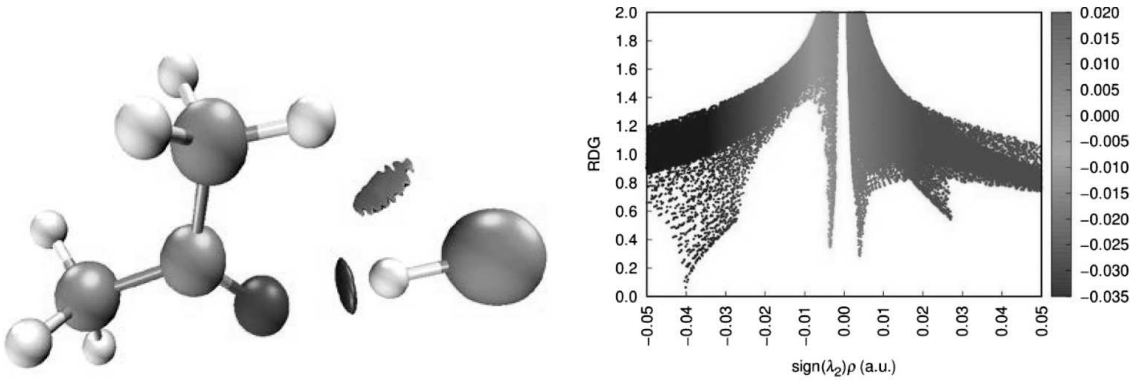

a *b*

Fig. 5. 3D colored isosurface (*a*) and 2D RDG graph of the acetone-HCl complex in Xe (*b*)

Table 3. **Spectral parameters of $(CH_3)_2CO\cdots HCl$ complexes in cryo-solutions**

Vibration	Q(C=O)			$\alpha^{+}_{CH_3}$(HCH)			Q^{-}(C–C)			νHCl		
	Exper.	Calculated		Exper.	Calculated		Exper.	Calculated		Exper.	Calculated	
		ν_h	ν_{anh}		ν_h	ν_{anh}		ν_h	ν_{anh}		ν_h	ν_{anh}
Gas	1742	1785	1761	1364	1385	1357	1218	1232	1200	2886	2927	2880
Free molecule												
Kr	1727	1775	1747	1368	1384	1352	1223	1233	1198	2861	2921	2875
Xe	1724	1772	1758	1372	1384	1351	1227	1233	1198	2848	2919	2873
Complex												
Kr	1713	1742	1706	1376	1389	1382	1238	1250	1221	2470	2476	2293
Xe	1710	1738	1702	1381	1389	1352	1241	1252	1215	2480	2448	2252

gen bonding and the weak van der Waals interactions, and blue patches ($\lambda_2(\rho) < -0.02$) signify strong electrostatic interactions.

For all studied compounds, blue regions appear, confirming the presence of hydrogen bonding between HCl and acetone in the $(CH_3)_2CO\cdots HCl$ complex. The 3D color map also highlights noncovalent dispersive forces within this complex (Fig. 3). RDG graphs further reveal that the intermolecular interaction energy (E_{int}) of the $(CH_3)_2CO\cdots HCl$ complex is stronger in krypton and xenon solvents than in vacuum (or gas phase). Additionally, the presence of more green patches between HCl and acetone in the complex suggests enhanced hydrogen bonding.

The NCI analysis of enantiomeric amino acid complexes reveals two key trends. First, it confirms the strong interactions between HCl and acetone in $(CH_3)_2CO\cdots HCl$. Second, increasing the size of the C=O group enhances acetone's selectivity and affinity due to the expanded carbonyl region.

It can be seen from the RGD graphs that the intermolecular interaction energy (E_{int}) of the $(CH_3)_2CO\cdots HCl$ complex is stronger in solvent Kr and Xe than in the gas state. In the case of the $(CH_3)_2CO\cdots HCl$ complex, more green patches were present between the HCl molecule and the acetone.

3.3. Experimental vibrational frequencies analysis

For relatively simple carbonyl-containing acceptors, numerous complexes with periodically varying interaction energies can be formed. IR absorption spectra of the $(CH_3)_2CO\cdots HCl$ complex and free $(CH_3)_2CO$ molecules in Kr and Xe solutions were registered. Table 3 presents the spectral properties of acetone bands that undergo noticeable shifts during hydrogen bond formation.

Compared to the gas phase, many bands exhibit low-frequency shifts in cryogenic solutions. Notably, the Q(C=O) band shifts by 15 cm^{-1} in Kr and

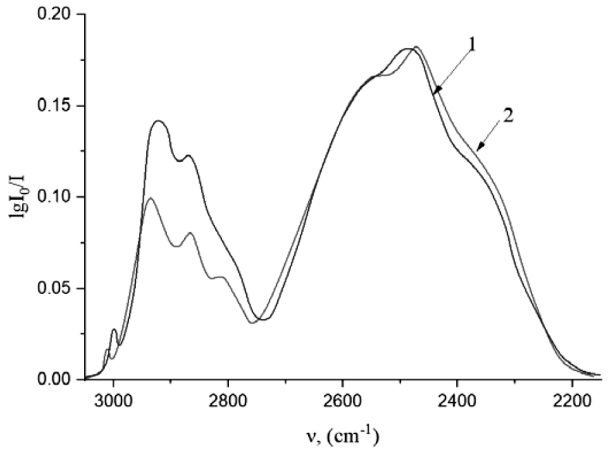

Fig. 6. IR spectra of $(CH_3)_2CO\cdots HCl$ complex in the region of νHCl band in inert solvents (concentration $(5+8)\times$ $\times 10^{-5}$ mol/l): *1* – in Kr at 160 K (blue line), *2* – in Xe at 170 K (red line)

18 cm^{-1} in Xe, with an accompanying half-width increase from 6 to 8 cm^{-1} in Xe. Additional low-frequency shifts are observed for q-(CH), q(CH), and q+(CH) bands, with maximum shifts reaching 15 cm^{-1} in Xe. Conversely, the α+(HCH) and Q(C–C) bands shift to higher frequencies by 4–5 cm^{-1} in Kr and 8–9 cm^{-1} in Xe.

Most proton donor and acceptor bands shift upon hydrogen bond formation. As expected for a hydrogen bond of this strength, the vHCl band undergoes a significant low-frequency shift, increased integral intensity, and a notable half-width expansion, distinguishing it from weaker complexes (Fig. 6) [33].

The primary objective of our computations was to characterize the experimental spectra in the ν(H–Cl) band area. Vibrational frequencies were calculated in harmonic and anharmonic approximations. It was observed that the ν(H–Cl) and ν(C=O) anharmonic frequencies of HCl and $(CH_3)_2CO$ molecules in the free state are closer to the vibrational frequencies obtained in the experiment (Table 3).

Figure 6 presents experimentally registered IR spectra of $(CH_3)_2CO\cdots HCl$ complex in the region of νHCl band in Kr and Xe solutions. It is seen that the band ν(H–Cl) of the complex in Kr solution is observed at 2470 cm^{-1}, while the corresponding vibrational frequency of the HCl molecule in the monomer state is ν_0(H–Cl) = 2861 ± 2 cm^{-1}. Due to the intermolecular interaction, the vibrational frequency of νHCl in the complex is shifted to-

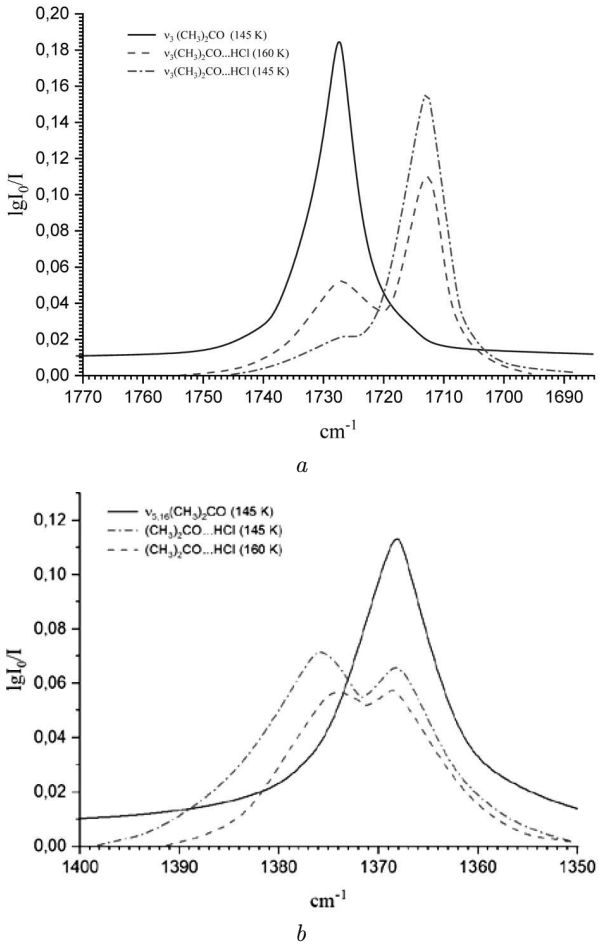

Fig. 7. IR spectra of $(CH_3)_2CO$ molecule and $(CH_3)_2CO\cdots HCl$ complex in Kr solution at different temperatures in the region of Q(C=O) band (*a*) and α_{CH_3}(HCH) vibration (*b*)

wards lower frequencies by $\Delta\nu$ = 391 cm^{-1}. In both Kr and Xe, the band of the complexly structured HCl complex is recorded around 2500 cm^{-1}; and a half-width of the band is approximately 250–300 cm^{-1}. The reason for the increased half-width of this band remains unresolved. In the Ar matrix, the complex's band is recorded at 2392 cm^{-1} [34]. Although the relative intensity of the side maxima differs, the $(CH_3)_2CO\cdots HCl$ complex exhibits a qualitatively similar pattern in both solutions. The most likely explanation for the side maxima is the coupling of vibrations with low-frequency stretching vibrations of the H-bond.

In solutions with Kr and Xe, a discrete shift and redistribution of the intensity on the acetone bands

is clearly recorded, both for the C=O vibration, directly involved in the formation of the hydrogen bond, and for the vibrations of the C-C and CH_3 groups. Figure 7, *a* shows the Q(C=O) band of the free $(CH_3)_2CO$ molecule and $(CH_3)_2CO\cdots HCl$ complex in Kr. For the free acetone molecule the band maximum is observed at 1727 cm^{-1}, for the complex it shifts to the low-frequency side to 1713 cm^{-1}; while the half-width of the band remains practically unchanged ($\Delta\nu_{1/2} \sim 6$ cm^{-1}).

The α_{CH_3}(HCH) band of the complex appears on the high-frequency side of the monomer band (Fig. 7, *b*) and shows no significant change in half-width. Although this group is not directly involved in hydrogen bond formation, its perturbation – evidenced by a shift relative to the monomer band – is identical to that of the C=O group. As temperature increases, the complexity of the bands also increases. In general, a significantly greater number of band alterations can be observed in solutions of liquefied noble gases compared to gaseous media or other solutions. Such measurements are particularly valuable for addressing vibrational challenges in hydrogen-bonded complexes.

4. Conclusions

In this study, we investigated the structure and vibrational properties of the $(CH_3)_2CO\cdots HCl$ complex using FTIR spectroscopy and density functional theory (DFT) calculations. The experimental and theoretical results provide valuable insights into the hydrogen bonding interactions in this system. The analysis was conducted in different environments, including vacuum, krypton (Kr), and xenon (Xe) solutions, allowing us to evaluate solvation effects on the structural and spectroscopic characteristics of the complex. The DFT calculations confirmed the formation of a stable hydrogen bond between the carbonyl oxygen of acetone and the hydrogen of HCl. The structural parameters obtained in vacuum and cryosolutions demonstrated small but significant changes due to solvation, with slight variations in bond lengths and angles. The interaction energy values indicated an increase in the hydrogen bond strength in the presence of Kr and Xe solvents compared to the gas phase. Topological analyses using Atoms in Molecules (AIM) theory and Non-Covalent Interaction (NCI) analysis further characterized the hydrogen bond nature. The AIM analysis confirmed the presence of a moderately strong hydrogen bond with partially covalent character, as evidenced by electron density values at the bond critical points. NCI analysis supported these findings, showing enhanced hydrogen bonding interactions in the solvent environments, with Kr and Xe strengthening the intermolecular interactions.

Experimental vibrational frequency analysis revealed noticeable shifts in the vibrational bands of both the acetone and HCl molecules upon complex formation. The IR spectra showed characteristic red shifts in the ν(HCl) stretching frequency, indicating significant hydrogen bond formation. Additionally, the shifts in the carbonyl stretching mode were consistent with the computational predictions. The good agreement between the experimental and theoretical spectra confirms the reliability of the computational approach used in this study.

Overall, our study provides a detailed characterization of the $(CH_3)_2CO\cdots HCl$ complex, highlighting the influence of solvation on hydrogen bonding interactions. These findings contribute to a deeper understanding of molecular interactions in hydrogen-bonded systems, which is essential for various applications in chemistry, biochemistry, and material sciences. Future studies could explore more complex hydrogen-bonded networks and investigate the dynamic behavior of such interactions using advanced spectroscopic techniques and molecular dynamics simulations.

1. O. Mishchuk, I. Doroshenko, V. Sablinskas, V. Balevicius. Temperature evolution of cluster structure in *n*-hexanol, isolated in Ar and N_2 matrices and in condensed states. *Struct. Chem.* **27**, 243 (2016).
2. E.N. Kozlovskaya, I. Doroshenko, V. Pogorelov, Ye. Vaskivsky, G.A. Pitsevich. Comparison of degrees of potential-energy-surface anharmonicity for complexes and clusters with hydrogen bonds. *J. Appl. Spectrosc.* **84**, 929 (2018).
3. I. Doroshenko, Ye. Vaskivskyi, Ye. Chernolevska, L. Meyliev, B. Kuyliev. Molecular isomerization in *n*-propanol dimers. *Ukr. J. Phys.* **65**, 291 (2020).
4. G.A. Pitsevich, E.N. Kozlovskaya, A.E. Malevich, I.Yu. Doroshenko, V.S. Satsunkevich, L.G.M. Pettersson. Some useful correlations for H-bonded systems. *Mol. Cryst. Liq. Cryst.* **696**, 15 (2020).
5. B. Golec, M. Mucha, M. Sałdyka, A. Barnes, Z. Mielke. Formaldoxime hydrogen bonded complexes with ammonia and hydrogen chloride. *Spectrochimica Acta Part A: Molecular and Biomolecular Spectroscopy* **136**, 68 (2015).
6. H.A. Hushvaktov, F.H. Tukhvatullin, A. Jumabaev, U.N. Tashkenbaev, A.A. Absanov, B.G. Hudoyberdiev,

B. Kuyliev. Raman spectra and ab initio calculation of a structure of aqueous solutions of methanol. *J. Mol. Struc.* **1131**, 25 (2017).
7. A. Jumabaev, U. Holikulov, H. Hushvaktov, A. Absanov, L. Bulavin, Interaction of valine with water molecules: Raman and DFT study. *Ukr. J. Phys.* **67**, 602 (2022).
8. D.S. Ahn, S.W. Park, I.S. Jeon, M.K. Lee, N.H. Kim, Y.H. Han, S. Lee. Effects of microsolvation on the structures and reactions of neutral and zwitterion alanine: Computational study. *J. Phys. Chem. B* **107**, 14109 (2003).
9. L. Yang, X. Liu, J. Zhang, J. Xie. Effects of microsolvation on a SN_2 reaction: Indirect atomistic dynamics and weakened suppression of reactivity. *Phys. Chem. Chem. Phys.* **19**, 9992 (2017).
10. A. Vasylieva, I. Doroshenko, Ye. Vaskivskyi, Ye. Chernolevska, V. Pogorelov. FTIR study of condensed water structure. *J. Mol. Struct.* **1167**, 232 (2018).
11. V. Balevicius, V. Sablinskas, I. Doroshenko, V. Pogorelov. Propanol clustering in argon matrix: 2D FTIR correlation spectroscopy. *Ukr. J. Phys.* **56**, 855 (2011).
12. V. Pogorelov, Ye. Chernolevska, Ye. Vaskivskyi, L.G.M. Pettersson, I. Doroshenko, V. Sablinskas, V. Balevicius, Ju. Ceponkus, K. Kovaleva, A. Malevich, G. Pitsevich. Structural transformations in bulk and matrix-isolated methanol from measured and computed infrared spectroscopy. *J. Mol. Liq.* **216**, 53 (2016).
13. W.O. George, B.F. Jones, R. Lewis, J.M. Price. Computations of medium strength hydrogen bonds–complexes of mono-and bi-functional carbonyl and nitrile compounds with hydrogen chloride. *Phys. Chem. Chem. Phys.* **2**, 4910 (2000).
14. H.D. Mettee, J. E. Del Bene, S. I. Hauck. An experimental and theoretical study of the thermodynamic properties of the acetone-hydrogen chloride complex. *J. Phys. Chem.* **86**, 5048 (1982).
15. D.S. Dudis, J.B. Everhart, T.M. Branch, S.S. Hunnicutt. Hydrogen bond energies of hydrogen chloride–carbonyl complexes. *J. Phys. Chem.* **100**, 2083 (1996).
16. J. Saikia, B. Borah, T.G. Devi. Study of interacting mechanism of amino acid and Alzheimer's drug using vibrational techniques and computational method. *J. Mol. Struc.* **1227**, 129664 (2020).
17. I. Singh, A.A. El-Emam, Sh.K. Pathak, R. Srivastava, V.K. Shukla, O. Prasad, L. Sinha. Experimental and theoretical DFT (B3LYP, X3LYP, CAM-B3LYP and M06-2X) study on electronic structure, spectral features, hydrogen bonding and solvent effects of 4-methylthiadiazole-5-carboxylic acid. *Mol. Simul.* **45**, 1029 (2019).
18. Y. Sert, L.M. Singer, M. Findlater, H. Dogan, C. Cirak. Vibrational frequency analysis, FT-IR, DFT and M06–2X studies on tert-Butyl N-(thiophen2yl)carbamate. *Spectrochim. Acta A Mol. Biomol. Spectrosc.* **128**, 46 (2014).
19. F. Akman, N. Issaoui, A.S. Kazachenko, Intermolecular hydrogen bond interactions in the thiourea/water complexes (Thio-$(H_2O)_n$) (n = 1, 5): X-ray, DFT, NBO, AIM, and RDG analyses. *J. Mol. Model.* **26**, 161 (2020).
20. M.J. Frisch, G.W. Trucks, H.B. Schlegel, G.E. Scuseria, M.A. Robb *et al.* Gaussian 09, Gaussian Inc, Wallingford CT, 2009.
21. R. Dennington, T. A. Keith, J. M. Millam. GaussView, Version 6.1, Semichem Inc., Shawnee Mission, KS, 2016.
22. T. Lu, F. Chen. Multiwfn: A multifunctional wavefunction analyzer. *J. Comput. Chem.* **33**, 580 (2012).
23. R.F.W. Bader. Atoms in molecules. *Acc. Chem. Res.* **18**, 9 (1985).
24. W. Humphrey, A. Dalke, K. Schulten. VMD: Visual molecular dynamics. *J. Mol. Graph.* **14**, 33 (1996).
25. Y. Bouteiller, Z. Latajka. Theoretical interpretation of acetone–HF infrared spectrum in the gas phase. *J. Chem. Phys.* **97**, 145 (1992).
26. V.P. Bulychev, K.G. Tokhadze. Comparative analysis of the H–F stretching band in absorption spectra of gas-phase complexes of HF with water, dimethyl ether, and acetone. *J. Mol. Struct.* **976**, 255 (2010).
27. T.M. Vilela, M.A. Gonçalves, R.C. Martins, M.J. Bazzana, A.A. Saczk, T.C. Ramalho, F.S. Felix. Solvent effects on the graphite surface targeting the construction of voltammetric sensors with potential applications in pharmaceutical area. *Electroanalysis* **35**, e202300075 (2023).
28. D. Tsering, P. Dey, T. Amin, A. Goswami, K.K. Kapoor, S.K. Seth. Combined experimental and theoretical studies of quinoxalinone-based spiropyrrolidines: Estimation of non-covalent interactions. *J. Mol. Struct.* **1318**, 139343 (2024).
29. C. Guerra, J. Burgos, L. Ayarde-Henríquez, E. Chamorro. Formulating reduced density gradient approaches for non-covalent interactions. *J. Phys. Chem. A* **128**, 6158 (2024).
30. A. B. Abraham, A. Y. Alzahrani, R. Thomas. Exploring non-covalent interactions between caffeine and ascorbic acid: Their significance in the physical chemistry of drug efficacy. *Zeitschrift für Physikalische Chemie* **238**, 401 (2024).
31. A. A. Basha, A. Kubaib, M. Azam. Exploring the antiviral potency of γ-FP and PA compounds: Electronic characterization, non-covalent interaction analysis and docking profiling with emphasis on QTAIM aspects. *Comp.Theor. Chem.* **1231**, 114412 (2024).
32. A. Rathika, V.J. Reeda, P. Divya. Synthesis, spectroscopic analysis (FT-IR, FT-Raman, UV, NMR), non-covalent interactions (RDG, IGM) and dynamic simulation on Bis (8-hydroxy quinoline) salicylate salicylic acid. *J. Mol. Struct.* **1310**, 138231 (2024).
33. A. Ramazani, M. Sheikhi, H. Yahyaei. Molecular structure, NMR, FMO, MEP and NBO analysis of ethyl-(Z)-3-phenyl-2-(5-phenyl-2H-1, 2, 3, 4-tetraazol-2-yl)-2-propenoate based on HF and DFT calculations. *Chem. Methodol.* **1**, e48 (2017).
34. A.J. Barnes. Molecular complexes of the hydrogen halides studied by matrix isolation infrared spectroscopy. *J. Mol. Struct.* **100**, 259 (1983).

Received 12.02.25

Г. Нурмуродова, І.Ю. Дорошенко,
Г. Муродов, У. Худжамов

ДОСЛІДЖЕННЯ ВОДНЕВО-ЗВ'ЯЗАНОГО КОМПЛЕКСУ $(CH_3)_2CO$–HCl МЕТОДАМИ FTIR СПЕКТРОСКОПІЇ ТА DFT

Вивчення комплексів з водневими зв'язками має вирішальне значення для розуміння міжмолекулярних взаємодій, які впливають на молекулярну структуру, розподіл електронної густини та коливальні властивості. У цій роботі ми досліджуємо комплекс ацетон-хлористого водню $(CH_3)_2CO$–HCl за допомогою інфрачервоної (ІЧ) фур'є-спектроскопії – Fourier transform infrared (FTIR) spectroscopy – у кріогенних розчинах криптону та ксенону, а також розрахунковим методом теорії функціонала густини (density functional theory, DFT). Експериментальні ІЧ спектри виявляють характерні зміщення частоти під час утворення комплексу, тоді як обчислювальний аналіз дає зрозуміти зміни геометричної та електронної структури. Топологічний аналіз, включно з методами атомів у молекулах (atoms in molecules, AIM) і нековалентної взаємодії (non-covalent interaction, NCI), підтверджує наявність і силу водневих зв'язків. Дослідження висвітлює вплив розчинника на коливальні властивості та міжмолекулярну взаємодію і покращує розуміння ролі водневих зв'язків у складних молекулярних системах.

Ключові слова: комплекс $(CH_3)_2CO$–HCl, ІЧ спектр, водневий зв'язок, FTIR спектроскопія, DFT, AIM, NCI.